A TWO-STAGE APPROACH TO SOLVING LARGE-SCALE OPTIMAL POWER FLOWS

Felix F. Wu* George Gross James F. Luini Pui Mee Look

Pacific Gas & Electric Company
San Francisco, California 94106

Abstract - A two stage optimization algorithm is developed for the solution of the large-scale optimal power flow (OPF) problem. The solution scheme is arrived at by exploiting the structural properties of the OPF problem formulation, including the physical characteristics of its variables. The algorithm incorporates certain features of the generalized reduced gradient and the penalty function methods. At each iteration a modified reduced gradient is used to provide a direction of movement. The use of penalty functions in the optimization is kept at a minimum. The generalized reduced gradient ideas are adapted in such a way that a routine power flow is used in the optimization. Numerical results of test cases including a 1410 bus system are given.

I. INTRODUCTION

The *optimal power flow* (OPF) problem is to minimize the fuel costs or some other quantities, e.g., system losses, taking into account the power flow constraints imposed by the transmission network together with other constraints such as real and reactive power generation limits and voltage magnitude limits. The OPF has been formulated as a nonlinear programming (NP) problem [1-6]. A number of NP techniques has been applied to the solution of the OPF problem. The use of the reduced gradient and the penalty function approach is reported in [1]. Application of the generalized reduced gradient (GRG) method to solve the OPF problem is given in [4]. In [5], the OPF problem is formulated as an unconstrained minimization problem using penalty functions and is solved using a Hessian matrix approach. The solution methodology of [6] makes use of an approximation to the Hessian. A comprehensive survey of the work in the OPF area is given by Happ [2] and Sasson and Merrill [3].

The size and the extensive amount of computation involved in solving the OPF problem for a power system with a thousand buses or more render it one of the largest NP problems. Our work on the OPF was undertaken with the view of developing a solution methodology to handle effectively such large scale optimizations. We have developed a two-stage optimization algorithm which is not a direct application of any standard NP techniques. Rather, we have derived our solution scheme by exploiting the structural properties of the OPF problem formulation, including the physical characteristics of its variables, and certain analytical properties of NP techniques. The optimization scheme combines a number of features of the GRG and penalty function methods while avoiding, to some extent, certain undesirable features of these methods.

The variables in the OPF problem are partitioned into dependent and independent variables with constraints on both groups of variables. In the first stage of the optimization algorithm most of the constraints on the dependent variables are ignored. Since virtually no use is made of penalty functions the first stage optimization converges fast. The second stage in which all constraints are included uses the solution of the first stage as the initial point to arrive at the optimal point. The iterative scheme of the two stages uses a modified reduced gradient at each iteration to provide a direction of movement. The use of penalty functions in the optimization is kept at a minimum. We have modified the ideas of the GRG method in such a way that a routine power flow is used in the optimization process. We have obtained very good results in our extensive testing of the two-stage optimization scheme.

We describe briefly the formulation of the OPF problem in the next section. We present a review of NP techniques pertinent to the solution of the OPF problem in Section III. We give an overview of the two-stage optimization algorithm in Section IV and discuss in detail its special features in the following section. We have implemented the optimization algorithm into a production grade program that can handle systems up to 2000 buses. Numerical results of some test cases including a 1410 bus system will be found in Section VI.

II. FORMULATION OF OPF PROBLEM

The formulation of the OPF problem used in this work is

minimize cost

subject to the equality constraints

(i) the power flow equations

and the inequality constraints on the

(ii) slack bus voltage magnitude V_s

(iii) slack bus real power P_s

(iv) voltage magnitude V_i at each PV bus i

(v) real power P_i at each PV bus i with variable generation

(vi) tap t of each load tap changing transformer

(vii) slack bus reactive power Q_s

(viii) reactive power Q_i at each PV bus i

(ix) voltage magnitude V_i at each PQ bus i

The power flow equations are a set of nonlinear equations

$$\underline{g}(\underline{x},\underline{u}) = \underline{0}$$

*Department of Electrical Engineering and Computer Sciences, University of California, Berkeley, CA 94720.

CH1318-3/79/0000-0126$00.75 © 1979 IEEE

The variables in the power flow equations are partitioned into the dependent variables $\underline{x}$ and the independent variables $\underline{u}$. The components of $\underline{u}$ and $\underline{x}$ are initially

$$\underline{u} = \begin{Bmatrix} V_s \\ P_j \text{ at PV bus j with variable generation} \\ V_j \text{ at PV bus j} \\ t \end{Bmatrix} \qquad \underline{x} = \begin{Bmatrix} P_s \\ Q_j \text{ at PV bus j} \\ V_{Rj}, V_{Ij} \text{ at each bus j except the slack bus} \end{Bmatrix}$$

The rectangular coordinate formulation of the power flow equation is used here. V_{Rj} and V_{Ij} denote the real and imaginary parts of the bus j voltage phasor, respectively.

Each inequality constraint (i) - (ix) restricts the range of values of a variable z_i and is of the form

$$z_i^m \le z_i \le z_i^M$$

where we use the superscripts m and M to denote the lower and upper limits of z_i.

The cost function defines the objective function which is to be minimized, e.g., the instantaneous production costs or the total system losses. An objective function depends directly on the system variables. We denote the cost function by $F(\underline{x},\underline{u})$.

The OPF problem can be expressed mathematically as

$$(A)\quad \begin{cases} \min F(\underline{x},\underline{u}) & (1) \\ \text{subject to} & \\ \underline{g}(\underline{x},\underline{u}) = \underline{0} & (2) \\ \underline{u}^m \le \underline{u} \le \underline{u}^M & (3) \\ \underline{x}^m \le \underline{x} \le \underline{x}^M & (4) \end{cases}$$

The formulation above is a *constrained nonlinear optimization problem*. In the section that follows we discuss the application of NP techniques to the OPF problem.

III. NONLINEAR OPTIMIZATION TECHNIQUES

Let us first consider the constrained optimization problem

$$(B)\quad \begin{cases} \min F(\underline{x},\underline{u}) \\ \text{subject to} \\ \underline{g}(\underline{x},\underline{u}) = \underline{0} \\ \underline{u}^m \le \underline{u} \le \underline{u}^M \end{cases}$$

We can solve (B) by using the reduced gradient method [7]. In this approach, each iteration consists of the following operations :

(i) Computation of the *reduced gradient* $\underline{r}$

$$\underline{r}^T = \frac{\partial F}{\partial \underline{u}} - \frac{\partial F}{\partial \underline{x}} \left(\frac{\partial \underline{g}}{\partial \underline{x}} \right)^{-1} \frac{\partial \underline{g}}{\partial \underline{u}} \qquad (5)$$

(ii) Determination of the descent direction $\Delta\underline{u}$ with components

$$\Delta u_i = \begin{cases} -r_i & \text{if } u_i^m < u_i < u_i^M \\ & u_i = u_i^M \text{ and } -r_i < 0 \\ & u_i = u_i^m \text{ and } -r_i > 0 \\ 0 & \text{otherwise} \end{cases} \qquad (6)$$

If $\Delta\underline{u} = 0$, then $\underline{u}$ is the optimal solution.

(iii) Selection of a stepsize $\hat{\alpha}$ along $\Delta\underline{u}$ by

a. finding the maximal value α_u such that

$$\underline{u}^m \le \underline{u} + \alpha_u \Delta\underline{u} \le \underline{u}^M$$

b. determining the stepsize $\hat{\alpha}$ which satisfies

$$F[\underline{x}(\underline{u}+\hat{\alpha}\Delta\underline{u}),\underline{u}+\hat{\alpha}\Delta\underline{u}] = \min_{\alpha} \{ F[\underline{x}(\underline{u}+\alpha\Delta\underline{u}),\underline{u}+\alpha\Delta\underline{u}] \mid 0 \le \alpha \le \alpha_u \} \qquad (7)$$

(iv) Construction of the new point $\underline{u}$

$$\underline{u} := \underline{u} + \hat{\alpha}\Delta\underline{u} \qquad (8)$$

Consider next the problem in which simple inequality constraints on the $\underline{x}$ variables, i.e., $\underline{x}^m \le \underline{x} \le \underline{x}^M$, are also included. This is the form of the OPF problem (A). The introduction of the constraints on $\underline{x}$ results in a considerably more complex problem than (B). Solution techniques that can handle (A) are classified as *indirect* and *direct* methods.

The *indirect* or *penalty function methods* transcribe the problem (A) into the form (B) by adding a penalty term to the cost function whenever a violation of

$$x_i^m \le x_i \le x_i^M \qquad (9)$$

occurs. The penalty term is a function of x_i: it is zero if (9) is satisfied and increases rapidly whenever x_i is outside its permissible range. Let $\pi_i(x_i)$ denote the *penalty term* for variable x_i. We define

$$\pi(\underline{x}) = \sum_i \pi_i(x_i)$$

to be the *penalty function* for inequality violations of $\underline{x}$ variables. The cost function in penalty function method becomes

$$\hat{F}(\underline{x},\underline{u}) = F(\underline{x},\underline{u}) + \mu\pi(\underline{x}) \qquad (10)$$

where μ is the so-called *penalty coefficient* and $\mu\pi(\underline{x})$ is the *penalty*. The solution obtained using the penalty function method converges to that of (A) as $\mu \to \infty$. The penalty function method has been applied to the OPF problem [1,5].

A major drawback in the actual implementation of the penalty function method is its slow convergence. We shall explain the reason for its slow convergence in what follows. The rate of convergence of the steepest-descent algorithm depends on the ratio η of the largest to the smallest eigenvalues of the Hessian matrix of the cost function ([7], p. 154). The higher the ratio η, the slower is the convergence. This effect is illustrated by the two-dimensional example shown in Fig. 1. The steepest-descent method converges more slowly as the contours of constant cost become more eccentric. Recall that for an ellipse η is the ratio of the major to the minor axis. Now, to solve (A) using the penalty function approach we minimize the function $\hat{F}(\underline{x},\underline{u})$ as defined in Eq. (10). If at the optimal solution of (A) there are k constraints that are active, i.e., are precisely at one of their limits, then k of the eigenvalues of the Hessian of $F(\underline{x},\underline{u}) + \mu\pi(\underline{x})$ will approach ∞ as $\mu \to \infty$ and the remaining eigenvalues will approach finite limits ([7], p. 287). Consequently the ratio $\eta \to \infty$. Thus in general we expect that the penalty function method will exhibit slow convergence.

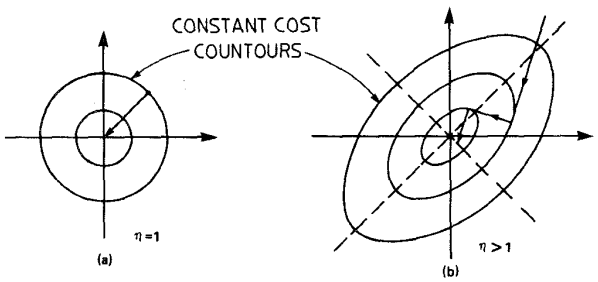

Fig. 1 The effect of the ratio η on the convergence of the steepest descent method.

In the class of *direct* or *primal* methods for solving (A) we first describe the *generalized reduced gradient* (GRG) technique. The GRG method starts with a feasible solution $(\underline{x}^o,\underline{u}^o)$. It then proceeds through the following steps:

(i) Computation of the reduced gradient $\underline{r}$ using eq.(5).

(ii) Computation of a descent direction $\Delta\underline{u}$ with components Δu_i given in eq. (6) If $\Delta\underline{u} = \underline{0}$, $\underline{u}$ is the optimal solution.

(iii) Computation of the corresponding change in $\underline{x}$ using linear approximation

$$\Delta\underline{x} = -\left(\frac{\partial \underline{g}}{\partial \underline{x}}\right)^{-1} \frac{\partial \underline{g}}{\partial \underline{u}} \Delta\underline{u}$$

(iv) Selection of a stepsize $\hat{\alpha}$ along $\Delta\underline{u}$ by

a. finding the maximal value α_u such that

$$\underline{u}^m \leq \underline{u} + \alpha_u \Delta\underline{u} \leq \underline{u}^M$$

b. finding the maximal value α_x such that

$$\underline{x}^m \leq \underline{x} + \alpha_x \Delta\underline{x} \leq \underline{x}^M$$

c. determining the stepsize $\hat{\alpha}$ which satisfies

$$F(\underline{x}+\hat{\alpha}\Delta\underline{x},\underline{u}+\hat{\alpha}\Delta\underline{u}) = \min_{\alpha} \{F(x+\alpha\Delta\underline{x},\underline{u}+\alpha\Delta\underline{u}) \Big| 0 \leq \alpha \leq \min(\alpha_u,\alpha_x)\} \quad (11)$$

(v) Construction of the new point

$\underline{u} := \underline{u} + \hat{\alpha}\Delta\underline{u}$

and solution for the new $\underline{x}$ satisfying

$\underline{g}(\underline{x},\underline{u}) = \underline{0}$

If $\underline{x}$ is feasible, the computation is returned to (i) to start a new iteration

(vi) If some component x_j of $\underline{x}$ is at one of its limits x_j^m or x_j^M, the variables $(\underline{x},\underline{u})$ are repartitioned. The x_j variable is made a $\underline{u}$ variable u_i and a $\underline{u}$ variable which is strictly within limits is made an $\underline{x}$ variable. This relabeling operation is carried out for each x_j variable at one of its limits. With the newly partitioned $(\underline{x},\underline{u})$ variable another iteration is started.

The partitioning scheme of step (vi) is essential in the proof of convergence of the algorithm. This scheme ensures that α_x is nonzero and consequently the GRG method will not stop because of the constraints on $\underline{x}$.

A major drawback of directly applying the GRG method to solve the OPF is the inability to incorporate a routine power flow solution as part of this approach. The reason for this is that there may arise an incompatibility between the partitioning scheme and the scheme and the structure of the load flow equations. Application of the GRG algorithm of the OPF has been reported in the literature [4]. However, only relatively small scale systems have been successfully handled by this approach.

We have developed an OPF solution methodology which makes detailed use of the structural properties of the OPF problem. We have modified the basic approach in the GRG scheme so that the power flow solution can be incorporated into each optimization iteration. We have taken into consideration the behavior of the OPF problem and the properties of various nonlinear optimization techniques in the development of the solution algorithm.

IV. TWO-STAGE OPTIMIZATION ALGORITHM

The approach to the solution of the OPF problem is in two stages. We give an overview of the algorithm in this section and leave to the next section a detailed discussion of the special features of the method.

First stage of the optimization algorithm. The first stage solves the problem

(P1): min cost

subject to

(i) power flow equations

(ii) slack bus V constraints

(iii) slack bus P constraints

(iv) V contraints at each PV bus

(v) P constraints at each PV bus with variable generation

(vi) t constraints at each variable tap transformer

At this stage the constraints (vii), (viii), and (ix) on the dependent variables Q_s, Q_i at PV bus i, and V_i at PQ bus i are not taken into account. These constraints will be considered subsequently.

We note that (P1) has the form of problem (A). However, (P1), without the inequalities (iii) on the slack bus active power P_s, takes on the form of problem (B). As discussed in Section III, problems of the form (B), can be solved using the reduced gradient method. We solve (P1) minus the constraints (iii) with a modified reduced gradient method. We handle the constraints (iii) by using the idea in the GRG scheme of limiting the stepsize α along the direction of movement. Should a zero stepsize result, however, the only change of variable permitted is the selection of a new slack bus. Computational aspects of the first stage algorithm are detailed in the next section.

We shall denote the solution obtained from the first stage by $(\underline{x}^{I*},\underline{u}^{I*})$. The first stage scheme does not take constraints (vii)-(ix) into account so that $(\underline{x}^{I*},\underline{u}^{I*})$ may not satisfy these constraints.

Interstage calculations. Before proceeding to the second stage solution scheme we modify the point $(\underline{x}^{I*},\underline{u}^{I*})$ to ensure that constraints (viii) on the reactive power Q_i at each PV bus i and (vii) on the slack bus reactive power Q_s are not violated. We check first for any Q violations at PV buses. Whenever such a violation occurs at a PV bus i, we set $Q_I = Q_i^{limit}$, where

$$Q_i^{limit} = \begin{cases} Q_i^M \text{ if upper limit of } Q_i \text{ is violated} \\ Q_i^m \text{ if lower limit of } Q_i \text{ is violated} \end{cases} \quad (12)$$

and switch bus status *temporarily* to PQ type. We then solve the power flow equations. The solution has the property that the Q constraints at all PV buses are satisfied. We next check whether Q_s lies in its permissible range. If a violation occurs we compute an estimate ΔV_s of the change in the voltage magnitude V_s at the slack bus which would bring Q_s within its allowable range. (For details see Appendix A). We then resolve the power flow equations with slack bus voltage magnitude $V_s + \Delta V_s$. At this point we restore the PV buses that have had temporary PQ status to their original PV status and proceed to the second stage.

Second stage of the optimization algorithm. In the second stage the problem (A) with all its constraints is considered. We take into account constraints (ix) on the voltage magnitude V_i at each PQ bus i by the penalty function approach. For each OPF iteration we compute the penalty function π defined by

$$\pi = \mu \sum_{\substack{i \text{ is a PQ bus} \\ \text{with voltage violation}}} (V_i - V_i^{limit})^2 \quad (13)$$

where

$$V_i^{limit} = \begin{cases} V_i^M & \text{if } V_i > V_i^M \\ V_i^m & \text{if } V_i < V_i^m \end{cases} \quad (14)$$

The second stage solves the problem

(P2): min {cost + π}
subject to

(i) power flow equations
(ii) slack bus V constraints
(iii) slack bus P constraints
(iv) V constraints at each PV bus
(v) P constraints at each PV bus with variable generation
(vi) t constraints at each variable tap transformer
(vii) slack bus Q constraints
(viii) Q constraints at each PV bus.

We use a modified reduced gradient approach to solve (P2). We handle the constraints of type (iii), (vii) and (viii) using the GRG technique idea of limiting the stepsize. The details including the switching of variables are given in the next section.

In the course of developing a solution methodology for the OPF problem we have observed from experiments with a large number of case studies that in the neighborhood of the optimal solution the cost function is flat, i.e., close to the optimal solution the cost function changes very little. This observation, in fact, led us to the idea of splitting the algorithm into two stages. The two-stage optimization algorithm first solves problem (P1). As such the solution $(\underline{x}^{I*}, \underline{u}^{I*})$ of (P1) provides a lower bound for the optimal solution of the OPF. Note that since (P1) contains fewer constraints, this problem is simpler to solve and the solution converges faster. Moreover, since there is no penalty function used the slow convergence characteristic of that method is avoided. Once the second stage algorithm is entered, we have a near optimal solution satisfying all constraints except possibly V constraints at PQ buses and/or PV buses. The solution obtained from the second-stage algorithm will satisfy all constraints except possibly the V constraints at some PQ buses.

V. FEATURES OF THE ALGORITHM

There are a number of special features embedded into the two-stage optimization scheme described in the previous section. These features are described in detail in this section.

Modification of the Direction of Movement

The basic idea of most iterative methods for solving nonlinear optimization problems is to generate at each iteration a new point at which the value of the cost function is lower. For this reason these methods are called descent methods. The reduced gradient method and the generalized reduced gradient method use the negative reduced gradient as the direction of descent. Locally, along this direction the value of the cost decreases the most. However, the direction along the negative reduced gradient may not be the "best" direction of descent from the global point of view. A typical example is shown in Fig. 2 for a two-dimensional unconstrained minimization problem. In general, the

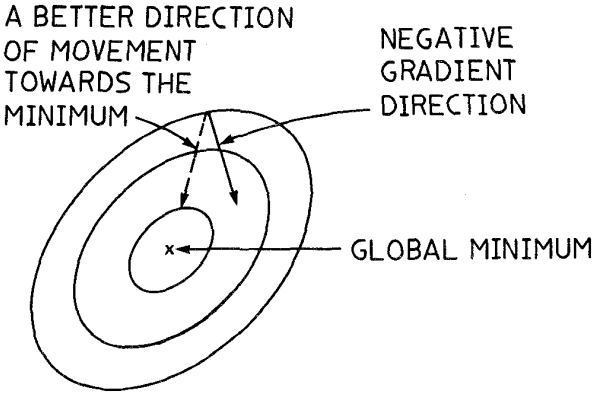

Fig. 2 Directions of movement for a two-dimensional example.

determination of a best direction of movement for a nonlinear programming problem is not possible. However, for special problems such as the OPF it is possible to establish some rules for the selection of an improved direction of movement. Based on certain physical considerations and on a series of extensive experiments we have developed two schemes for the construction of a modified and improved direction of movement.

a. Elimination of Zigzagging

In our use of the reduced gradient algorithm for the solution of OPF problem we have frequently observed the following phenomenon: the solution trajectory hits one of the constraint boundaries again and again in successive iterations without achieving a substantial decrease in the value of the cost function. This so-called *zigzagging* may be eliminated to some extent by damping one or more components of the direction of movement. Suppose that at a particular iteration we are close to one or more boundaries imposed by the OPF problem constraints. In such a case we decrease those components of the direction of movement that point towards one of these constraint boundaries. This decrease is implemented by using the *damping factor* d_i to compute the ith component of the modified direction of movement. Thus after computing the reduced gradient $\underline{r}$ (see eq. (5), for example) we calculate

$$d_i = \begin{cases} u_i^M - u_i \text{ if } u_i^m \le u_i \le u_i^M \text{ and } r_i < 0 \\ u_i - u_i^m \text{ if } u_i^m \le u_i \le u_i^M \text{ and } r_i > 0 \end{cases} \quad (15)$$

We compute the components of the modified direction of movement.

$$\Delta u_i = -d_i r_i \quad (16)$$

The effect of this damping mechanism for a two-dimensional example is illustrated in Fig. 3. We can see that such damping may improve convergence. For the OPF problem the implementation of the modified direction of movement using damping factor d_i has eliminated the zigzagging phenomenon to some extent and has markedly improved convergence: cases that failed to converge using the negative reduced gradient direction now do, and in other cases the number of iterations has been reduced. Based on our extensive experiments, we concluded that for greatest effectiveness the use

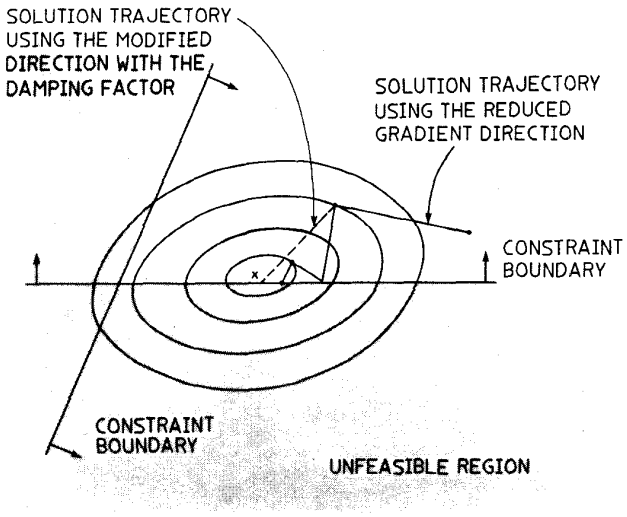

Fig. 3 Modified direction of movement by means of the damping factor.

of the damping factor should be limited to the $\underline{u}$ components corresponding to voltages at PV buses or taps of variable tap transformers.

b. Scaling of Components

The independent $\underline{u}$ variables may be classified into two groups: $\underline{u1}$, consisting of power variables -- real or reactive, and $\underline{u2}$ consisting of voltages or taps. The change in the value of the cost function corresponding to a per unit change in a component of $\underline{u1}$ may be very different from that corresponding to a per unit change in a component of $\underline{u2}$. Consequently the ratio η of the largest to the smallest eigenvalue of the Hessian matrix of the cost function may be much greater than one. For the simple case of scalar ul and scalar u2 we may have eccentric cost contours as shown in Fig. 4(a) or 4(b). As we mentioned earlier in Section III a large η results in slow convergence. In our attempt to improve the convergence of the solution algorithm, we have introduced a *scaling ratio* s by which we multiply each component of $\underline{u2}$. The rationale for the use of the scaling ratio is to introduce a change of variables that would lead to a more favorable eigenvalue structure in the Hessian of the cost function (i.e., with ratio η closer to 1).

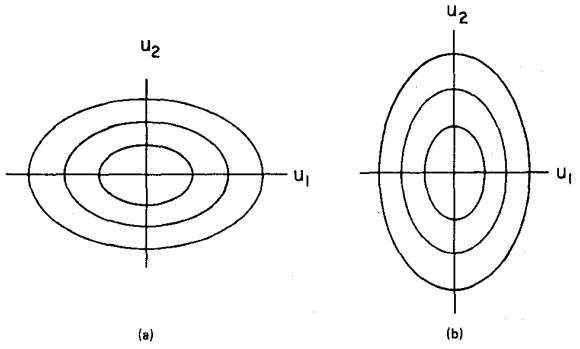

Fig. 4 Possible cost contours for the two-dimensional case.

The use of the scaling ratio s has been found effective in enhancing the convergence characteristics of the optimization scheme. We have found cases that even with the use of the damping factor failed to converge, yet with an appropriate choice of s convergence is obtained within a reasonable number of iterations.

The Linear Search Subproblem

At each iteration of the optimization scheme, once the direction of movement is known the stepsize $\hat{\alpha}$ that we move along that direction must be determined. The stepsize $\hat{\alpha}$ is selected so that we move to a relative minimum of the cost function along the direction of movement. The stepsize selection is determined by finding an approximation to the solution of this one dimensional minimization known as the *linear search subproblem*.

We have experimented with a number of linear search subproblem solution schemes for the OPF including those used for the Newton load flow [8]. We have found the well-known Devidon Cubic Interpolation Method [9] to be most effective. This technique uses the values of the cost function and its derivative at two points on the direction of movement to determine $\hat{\alpha}$. Let

$$\psi(\alpha) = F[\underline{x} + \alpha\Delta\underline{x},\ \underline{u} + \alpha\Delta\underline{u}] \quad (17)$$

be the value of the cost along the direction of movement. Suppose that α^M denotes the maximum value that α may take so that the inequality constraints $\underline{u}^m \le \underline{u} + \alpha\Delta\underline{u}^M$ and $\underline{x}^m \le \underline{x} + \alpha\Delta\underline{x} \le \underline{x}^M$ are satisfied. Using the quantities $\psi(0) = F(\underline{x},\underline{u})$, $\psi'(0) = \left.\frac{d\psi}{d\alpha}\right|_{\alpha=0} = \left.\frac{dF}{d\alpha}\right|_{(\underline{x},\underline{u})}$, $\psi(\alpha^M) = F[\underline{x}+\alpha^M\Delta\underline{x},\underline{u}+\alpha^M\Delta\underline{u}]$, and $\psi'(\alpha^M) = \left.\frac{dF}{d\alpha}\right|_{(\underline{x}+\alpha^M\Delta\underline{x},\underline{u}+\alpha^M\Delta\underline{u})}$ we fit a cubic through the two points with the corresponding slopes (see Fig. 5). The minimum of the cubic curve is readily computed:

$$\hat{\alpha} = \alpha^M - \alpha^M \frac{\psi'(\alpha^M) + w - v}{\psi'(\alpha^M) - \psi'(0) + 2w} \quad (18)$$

where,

$$w = [v^2 - \psi'(0)\psi'(\alpha^M)]^{1/2}$$

$$v = \frac{3}{\alpha^M}[\psi(0) - \psi(\alpha^M)] + \psi'(0) + \psi'(\alpha^M) \quad (19)$$

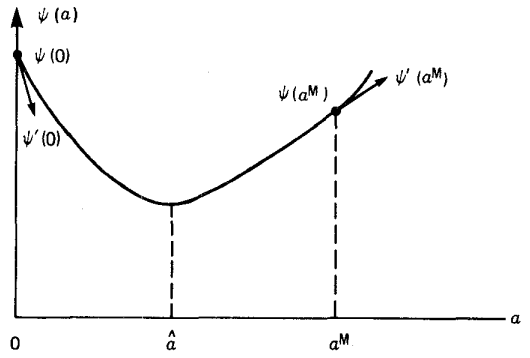

Fig. 5 The Davidon cubic interpolation method.

Transformer Taps

In the OPF formulation a transformer with a variable tap is used to maintain the voltage on one side of the transformer (either the high or the low side) within a prescribed range by adjusting the tap. In the OPF solution scheme we treat each tap t of a variable tap transformer as a $\underline{u}$ variable. Given an initial value for t, we solve the load flow equations and compute the reduced gradient as in eq. (5). We associate each tap t with the line which connects the two buses on either of its sides. Thus in the matrix of partial derivatives $\partial g/\partial \underline{u}|(\underline{x},\underline{u})$, for each t variable there are entries in the rows corresponding to the equations for the two buses. Once the direction of movement $\Delta\underline{u}$ and the stepsize $\hat{\alpha}$ are determined, we repeat this process in the next OPF iteration with the new value $t + \hat{\alpha}\Delta t$ for each tap.

The Handling of Constraints on $\underline{x}$ Variables

In the first stage of the optimization scheme, the only $\underline{x}$ constraints considered are those on the slack bus real power.

(a) Slack bus real power constraints

We make use of the penalty function idea to "force" the real power injection at the slack bus P_s to move within its limits

$$P_s^m \leq P_s \leq P_s^M \tag{20}$$

whenever P_s is outside of its limits. To do this we modify the cost curve associated with a generator used as a slack bus in such a way that very high costs are assigned whenever the real power of the generator is outside its permissible range. An example of a modified input-output curve for a slack bus actually used in a 1410 bus test system is given in Fig. 6.

In addition, at each OPF iteration we ensure that the new point that we construct will have the slack bus real power within its limits. The change $\Delta\underline{u}$ in $\underline{u}$ causes a change ΔP_s. In limiting the stepsize α along the direction of movement, we ensure that $P_s + \alpha\Delta P_s$ remains within its limits. The exact value of ΔP_s can be obtained only from a power flow solution. However, we may easily obtain an approximation of ΔP_s using the linearized power flow equations (see Appendix A). This is the stepsize limitation idea of the GRG method. We pick the stepsize limit α_{P_s} by taking the largest value of α that satisfies

$$P_s^m \leq P_s + \alpha\Delta P_s \leq P_s^M \tag{21}$$

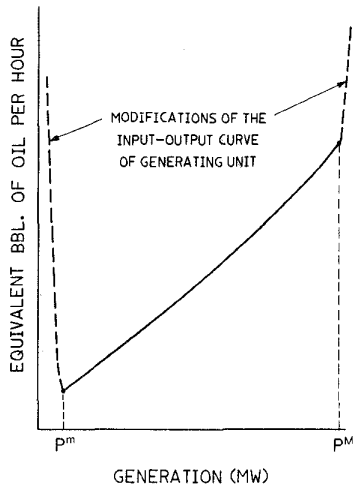

Fig. 6 Modified cost curve associated with a slack bus.

It may happen that α_{P_s} is very close to zero, so that no movement along $\Delta\underline{u}$ direction is possible. In this case a new slack bus is picked. The load flow equations are solved again and the reduced gradient is recomputed with the newly selected slack bus. The iterative process then continues.

(b) Q constraints at PV buses

The constraints on Q_i at each PV bus i are handled in the second stage optimization using the stepsize limitation idea of the GRG method. We compute the change ΔQ_i in Q_i corresponding to the change $\Delta\underline{u}$ in $\underline{u}$ along the direction of movement using a linearized relation. Let α_{Q_i} be the maximum value of α so that

$$Q_i^m \leq Q_i + \alpha\Delta Q_i \leq Q_i^M$$

If α_{Q_i} is very close to zero we make the following change of variables: we remove V_i as a $\underline{u}$ variable and replace it by Q_i with its value set at Q_i^{limit} given in eq. (12) and switch bus i to PQ bus status *permanently*. We recompute the reduced gradient $\underline{r}$ and the direction of movement $\Delta\underline{u}$ and repeat the stepsize selection process.

(c) Slack bus reactive power constraints

In the second stage optimization, the constraints

$$Q_s^m \leq Q_s \leq Q_s^M$$

are treated similarly to the Q constraints at PV buses. Using linearization we compute the change ΔQ_s in Q_s corresponding to the change $\Delta\underline{u}$ in $\underline{u}$. Let α_{Q_s} be the limiting value of α so that

$$Q_s^m \leq Q_s + \alpha\Delta Q_s \leq Q_s^M$$

is satisfied. If α_{Q_s} is very close to 0, then we make the following changes: we set $Q_s = Q_s^{limit}$, switch the bus to permanent PQ status and select a new slack bus. Q_s^{limit} is the value of the limit of Q_s which limits the stepsize. We then solve the load flow equations, recompute the reduced gradient and the direction of movement with the new slack bus and repeat the stepsize selection process.

(d) V constraints at PQ buses

In the second stage of the optimization scheme we consider violations of the voltage limits at PQ buses. These include the original PQ buses, the PQ buses switched from PV buses as described in (b), and the PQ buses which were previously slack buses as described in (c). If the load flow solution is such that for a PQ bus a voltage magnitude constraint is violated, then a penalty term is added to the cost function. On the other hand, if for a PQ bus i V_i is within its $[V_i^m, V_i^M]$ range, then we use the stepsize limitation idea to handle this contraint. Corresponding to the direction of movement $\Delta\underline{u}$ we compute the change ΔV_i in the voltage magnitude using a linearization-based relationship. Let α_{Vi} be the maximum value of α with which the constraint

$$V_i^m \leq V_i + \alpha\Delta V_i \leq V_i^M$$

is satisfied. If α_{Vi} is close to zero then we introduce V_i as a $\underline{u}$ variable with its value set at its limiting value and switch bus i to PV status on a *temporary* basis. We then recompute the reduced gradient and the direction of movement and repeat the stepsize selection process, after which bus i is restored to PQ status. The reason for this temporary PV-PQ status switching is to obtain a different direction of movement when we are in a deadlock situation.

The stepsize α^M used in the linear search subproblem in each OPF iteration is the minimum of α_{Ps}, α_{Qs}, α_{Vj} and α_u. Once $\hat{\alpha}$ is determined we construct the new point $\underline{u} + \hat{\alpha}\Delta\underline{u}$. We use $\underline{x} + \hat{\alpha}\Delta\underline{x}$ as a starting point for the power flow equations in the next iteration. Usually one iteration is sufficient for the power mismatches in the power flow to be reduced within the preset tolerance.

VI. NUMERICAL RESULTS

We have tested the two-stage optimization algorithm on a large number of systems with sizes ranging from 11 buses to up to 1500 buses. For the purpose of this paper we restrict our attention to four test systems. Their characteristics are given in Table I. In our testing we have used a wide variety of system conditions.

TABLE I: CHARACTERISTICS OF THE TEST SYSTEMS

Characteristic	System A	System B	System C	System D
Number of buses	11	136	333	1410
Number of lines	13	197	484	1840
Number of PV buses	7	33	70	141
Number of buses with variable real power generation	4	14	17	27
Number of variable tap transformers	0	5	21	82

We have tabulated data concerning the computational characteristics of the optimization method which are typical for the four systems in Table II. All computation times are for an IBM 370/168. It is interesting to note that the optimization calculations in both stages of the algorithm for an OPF iteration excluding the power flow solution are of the same order of magnitude as a power flow iteration. The data in Table II clearly shows that the majority of the time in the optimization is taken up by the power flow iterations. A plot of the total CPU times to solve the OPF vs. system size is given in Fig. 7.

We next consider some of the specific characteristics of the performance of the optimization method on the test systems. The plot in Fig. 8 of the system cost for each OPF iteration is typical of the behavior of the cost function in the two stages of the optimization. In the first stage the cost function decreases rapidly in each successive OPF iteration. The first stage optimization converges in 18 iterations at a point we call $(\underline{x}^{I*}, \underline{u}^{I*})$. The lower bound for the optimal solution to the OPF is the cost at $(\underline{x}^{I*}, \underline{u}^{I*})$ and is indicated by point A. The main goal in the calculations following convergence in the first stage is to modify the solution so that no Q violations at generator buses and V viola-

TABLE II: COMPUTATIONAL CHARACTERISTICS OF THE TWO-STAGE OPTIMIZATION SCHEME

		System A	System B	System C	System D
	time for one load flow iteration (CPU sec)	.015	.12	.35	2
FIRST STAGE	total number of load flow iterations	46	32	55	61
	total number of OPF iterations	11	12	13	18
	time for optimization computations except load flow solution in an OPF iteration (CPU sec)	.06	.11	.35	1.6
	total time (CPU sec)	-	6.95	26.4	160
INTER-STAGE	total number of load flow iterations to satisfy Q constraints	2	4	3	5
SECOND STAGE	total number of load flow iterations	does not go through the second stage	6	83	46
	total number of OPF iterations		2	21	26
	minimum and maximum time for optimization calculations except load flow solution in an OPF iteration		.11 .31	0.8 1.2	1.8 7.35
	total computation time (CPU sec)	2.1	10.4	80	380

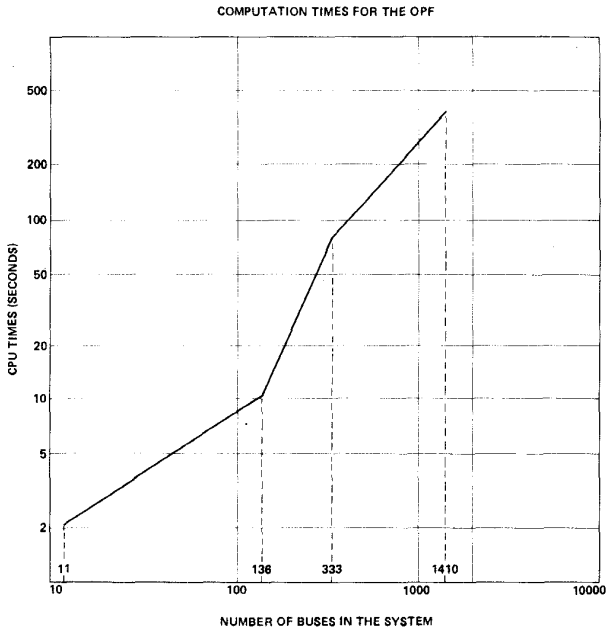

Fig. 7 Computation time of the optimization scheme as a function of system size.

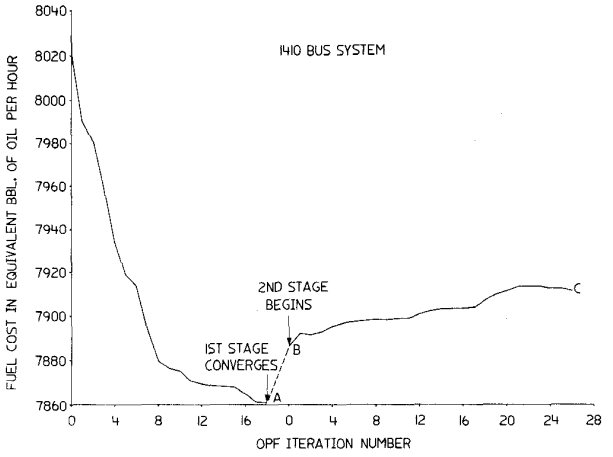

Fig. 8 Behavior of the System D cost function in the two-stage optimization scheme.

tions at PQ buses occur. We note that the cost increases as we modify $(\underline{x}^{I*},\underline{u}^{I*})$ to satisfy Q constraints (point B). At the initial point of the second stage there are violations of the constraints on the voltage magnitude at 101 PQ buses. The penalty function π (the sum of the squares of the voltage magnitude violations) at this point has a value of 2.24×10^{-2}. After 26 iterations all violations except those of voltage magnitude at 21 PQ buses have been removed with only a slight increase of the cost (point C). The penalty function π has been reduced to 1.6×10^{-4}. Note that while the cost may increase in certain iterations of the second stage, the number of PQ buses at which voltage magnitude violations occur decreases in each iteration. A plot of the modified cost function for System D is given in Fig. 9.

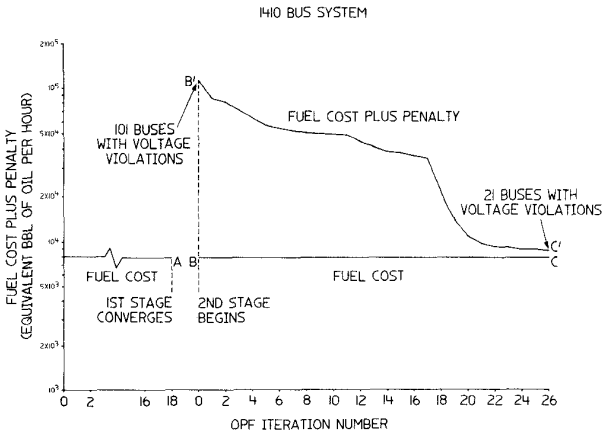

Fig. 9 Behavior of the modified cost function for the second stage of the optimization scheme ($\mu = 5 \times 10^6$).

In our testing we have studied the effects of the value of the penalty coefficient μ. Our results indicate that the behavior of the solution scheme is insensitive to the choice of μ. The results tabulated in Table III are from a set of tests on System D with system conditions that are different from those for which the data for Figs. 8 and 9 were obtained. These

TABLE III: THE EFFECT OF THE PENALTY COEFFICIENT μ FOR SYSTEM D

μ	Ratio*	The value of π after iteration			
		4	8	12	15
10^5	.0223	10.37×10^{-4}	9.6×10^{-4}	6.2×10^{-4}	5.46×10^{-4}
2×10^6	.446	9.87×10^{-4}	7.23×10^{-4}	5.44×10^{-4}	5.02×10^{-4}
5×10^6	1.115	9.89×10^{-4}	6.86×10^{-4}	4.9×10^{-4}	3.55×10^{-4}
10^7	2.23	9.89×10^{-4}	5.91×10^{-4}	5.0×10^{-4}	4.2×10^{-4}

*Ratio $= \frac{\mu\pi}{F}$ with π and F evaluated at the initial point of the second stage ($\pi = 17.7\times10^{-4}$, F = 7928)

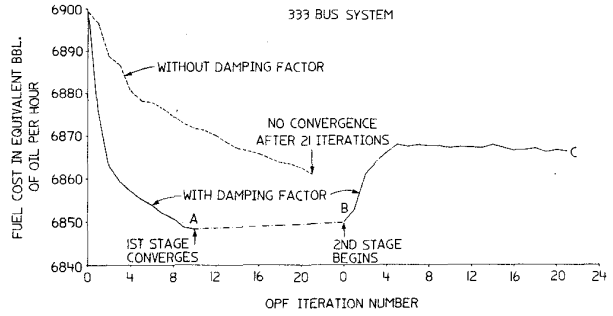

Fig. 10 Effect of the use of the damping factor for System C.

results, however, are typical.

Many cases for which the method using the (pure) reduced gradient direction fails to converge do con-

verge when the direction is modified by the damping factor. For example for System C we can see from Fig. 10 that in the first stage without the damping factor we have no convergence after 21 iterations while with the damping factor we obtain convergence in 18 iterations. Note that after the first stage the behavior of the System C cost function is very similar to that of System D in Fig. 8.

We note, however, that even with the use of the damping factor we may have no convergence when an inappropriate choice of the scaling ratio is used. This is the case for System D as shown in Fig. 11. With a choice of scaling ratio s = 0.5, we obtain convergence. A similar situation arises for System C for which we have no convergence with s = 0.1 and convergence with s = 1,2 and 5, as shown in Fig. 12. It is interesting to note that while in the first stage with different scaling ratios the optimization converges to different lower bounds, in the second stage the three values of s result in virtually the same cost.

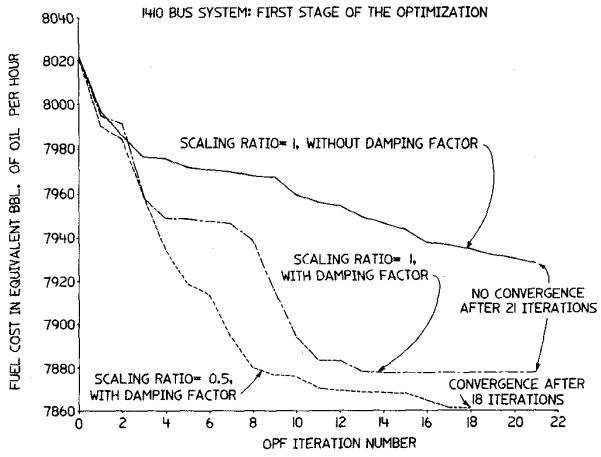

Fig. 11 The effects of the damping factor and the scaling ratio for the first stage optimization for System D.

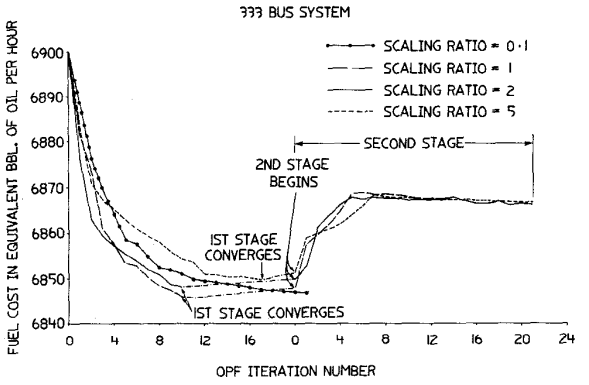

Fig. 12 Behavior of the cost function for different scaling ratios for System C.

VII. CONCLUSION

We have presented a two-stage optimization algorithm for the solution of large-scale power flow problems. A noteworthy feature of the solution scheme is the effective manner in which the constraints on the dependent variables are handled. This is done by keeping the use of penalty functions at a minimum and by applying the stepsize limitation idea of the GRG. The switching of variables which is intrinsic to the GRG technique is modified so as to make it compatible with the power flow formulation. This aspect has the important consequence that a routine power flow can be incorporated in the optimization. From extensive testing of the optimization algorithm, we condcluded that it deals effectively with large systems. An extension of the work reported here is the application of the OPF optimization scheme to the solution of the var allocation problem.

VIII. REFERENCES

[1] H.W. Dommel and W.F. Tinney, "Optimal power flow solutions," IEEE Trans. Power Apparatus and Systems, Vol. PAS-87, pp. 1866-1876, October 1968.

[2] H.H. Happ, "Optimal power dispatch -- a comprehensive survey," IEEE Trans. Power Apparatus and Systems, Vol. PAS-96, pp. 841-854, May/June 1977.

[3] A.M. Sasson and H.M. Merrill, "Some applications of optimization techniques to power system problems," Proc. IEEE, Vol. 62, pp. 959-972, July 1974.

[4] J. Peschon, D.W. Bree and L.P. Hajdu, "Optimal solutions involving system security," 1971 PICA Conf. Proc., pp. 210-218, 1971.

[5] A.M. Sasson, F. Viloria, and F. Aboytes, "Optimal load flow solution using the Hessian matrix," IEEE Trans. Power App. Syst., Vol. PAS-92, pp. 31-41, January/February 1973.

[6] W.R. Barcelo, W.W. Lemmon and H.R. Koen, "Optimization of the real-time dispatch with constraints for secure operation of bulk power systems," IEEE Trans. Power Apparatus and Systems, Vol. PAS-96, pp. 741-757, May/June 1977.

[7] D.G. Luenberger, Introduction to Linear and Nonlinear Programming, Addison-Wesley Publishing, Company, Reading, Massachusetts, 1973.

[8] G. Gross and J.F. Luini, "Effective control of convergence of the Newton load flow," TP II-A, 1975 PICA Conf. Proc., pp. 41-48, 1975.

[9] W.C. Davidon, "Variable metric method for minimization," AEC Research and Development Rept. ANL-5990 (rev.), Argonne National Laboratories, 1959.

IX. APPENDIX A: COMPUTATION OF Δx

To compute an approximation of the change in a dependent variable caused by the change Δu in the independent variable u we use the linearized form of the power flow equations (2). Thus Δx is the solution of the linear system

$$\left(\frac{\partial g}{\partial x}\right)\Delta x = -\left(\frac{\partial g}{\partial u}\right)\Delta u \qquad \text{(A1)}$$

Computation of ΔP_s. We partition the x and u variables as $x = (P_s, \hat{x}^T)^T$ and $u = (V_s, \hat{u}^T)^T$ where $\hat{x}$ and $\hat{u}$ are the dependent and independent variables, respectively, at all the buses except the slack bus. We rewrite (2) as

$$g(x,u) = \begin{bmatrix} P_s - g_s(\hat{x}, V_s, \hat{u}) \\ \hat{g}(\hat{x}, V_s, \hat{u}) \end{bmatrix} = \begin{bmatrix} 0 \\ \hat{0} \end{bmatrix} \qquad \text{(A2)}$$

and (A1) as

$$\left[\begin{array}{c|c} 1 & -\frac{\partial g_s}{\partial \hat{x}} \\ \hline \underline{0} & \frac{\partial \underline{\hat{g}}}{\partial \underline{\hat{x}}} \end{array}\right]\left[\begin{array}{c} \Delta P_s \\ \hline \Delta \underline{\hat{x}} \end{array}\right]=\left[\begin{array}{c|c} \frac{\partial g_s}{\partial V_s} & \frac{\partial g_s}{\partial \underline{\hat{u}}} \\ \hline \frac{\partial \underline{\hat{g}}}{\partial V_s} & \frac{\partial \underline{\hat{g}}}{\partial \underline{\hat{u}}} \end{array}\right]\left[\begin{array}{c} \Delta V_s \\ \hline \Delta \underline{\hat{u}} \end{array}\right] \tag{A3}$$

Then

$$\Delta P_s = \left[\frac{\partial g_s}{\partial V_s} - \frac{\partial g_s}{\partial \underline{\hat{x}}}\left(\frac{\partial \underline{\hat{g}}}{\partial \underline{\hat{x}}}\right)^{-1}\frac{\partial \underline{\hat{g}}}{\partial V_s}\right]\Delta V_s + \left[\frac{\partial g_s}{\partial \underline{\hat{u}}} - \frac{\partial g_s}{\partial \underline{\hat{x}}}\left(\frac{\partial \underline{\hat{g}}}{\partial \underline{\hat{x}}}\right)^{-1}\frac{\partial \underline{\hat{g}}}{\partial \underline{\hat{u}}}\right]\Delta \underline{\hat{u}} \tag{A4}$$

is the relation used for approximating the change in P_s corresponding to the change $\Delta \underline{u}$ in $\underline{u}$.

Computation of ΔQ_s. Let

$$Q_s = q_s\ (\underline{\hat{x}}, V_s, \underline{u}) \tag{A5}$$

Then, based on linearization

$$\Delta Q_s = \left[\frac{\partial q_s}{\partial V_s} - \frac{\partial q_s}{\partial \underline{\hat{x}}}\left(\frac{\partial \underline{\hat{g}}}{\partial \underline{\hat{x}}}\right)^{-1}\frac{\partial \underline{\hat{g}}}{\partial V_s}\right]\Delta V_s + \left[\frac{\partial q_s}{\partial \underline{\hat{u}}} - \frac{\partial q_s}{\partial \underline{\hat{x}}}\left(\frac{\partial \underline{\hat{g}}}{\partial \underline{\hat{x}}}\right)^{-1}\frac{\partial \underline{\hat{g}}}{\partial \underline{\hat{u}}}\right]\Delta \underline{\hat{u}} \tag{A6}$$

is the relation used for approximating the change in Q_s corresponding to the change $\Delta \underline{u}$ in $\underline{u}$.

Special case. If Q_s violates one of its limits for the solution obtained in the first stage optimization, in the interstage computations we must determine the change ΔV_s in V_s that would cause Q_s to move into its permissible range. Thus

$$\Delta Q_s = Q_s^{limit} - Q_s$$

and since $\Delta \underline{u} = \underline{0}$, Eq. (A6) reduces to

$$\Delta Q_s = \left[\frac{\partial q_s}{\partial V_s} - \frac{\partial q_s}{\partial \underline{\hat{x}}}\left(\frac{\partial \underline{\hat{g}}}{\partial \underline{\hat{x}}}\right)^{-1}\frac{\partial \underline{\hat{g}}}{\partial V_s}\right]\Delta V_s \tag{A7}$$

We use (A7) to compute ΔV_s in the interstage phase of the optimization scheme.

X. APPENDIX B: OPTIMIZATION ALGORITHM

First stage: start with an initial point $\underline{u}^o$.

I-1 Initialization: Solve for $\underline{x}^o$ in the power flow equations (2) with $\underline{u} = \underline{u}^o$; set $k = 0$

I-2 Computation of the reduced gradient $\underline{r}$: Evaluate $\underline{r}$ at $(\underline{x}^k, \underline{u}^k)$ using eq. (5).

I-3 Convergence check: If

$$\begin{cases} r_i > -\varepsilon_1 & \text{for } u_i = u_i^m \\ |r_i| < \varepsilon_1 & \text{for } u_i < u_i < u_i^M \\ r_i < \varepsilon_1 & \text{for } u_i = u_i^M \end{cases}$$

the first stage converges; else, go to I-4.

I-4 Computation of the direction of movement $\Delta \underline{u}$: Evaluate the components

$$\Delta u_i = \begin{cases} -r_i * d_i & \text{if } u_i \text{ is a component of } \underline{u2} \\ -r_i * s & \text{if } u_i \text{ is a component of } \underline{u1} \end{cases}$$

where d_i is the damping factor and s is the scaling ratio.

I-5 Computation of stepsize limit: Find the maximum value α_u of α that satisfies $\underline{u}^m \le \underline{u}^k + \alpha\Delta\underline{u} \le \underline{u}^M$; compute ΔP_s using linearization and find α_{Ps} the limiting value of α so that relation (21) is satisfied.

I-6 Slack bus selection: If $|\alpha_{Ps}\ \Delta P_s| < 0.05\ P_s^{limit}$ where P_s^{limit} is that value of P_s that limits the stepsize, pick a new slack bus, solve the load flow equations and go to I-2; else go to I-7.

I-7 Line search: Find $\hat{\alpha}$ that minimizes $F(\underline{x}^k + \alpha\Delta\underline{x}, \underline{u}^k + \alpha\Delta\underline{u})$ in the interval $0 < \alpha < \min(\alpha_{Ps}, \alpha_u)$.

I-8 Update: Set $\underline{u}^{k+1} = \underline{u}^k + \hat{\alpha}\Delta u$, $\underline{x}^{k+1} = \underline{x}^k + \hat{\alpha}\Delta x$, $k = k+1$, solve the laod flow equations and go to I-2.

Second stage: Start with the modified solution $(\underline{x}^o, \underline{u}^o)$ of the first stage following interstage calculations.

II-1 Initialization: Same as I-1

II-2 Computation of $\underline{r}$: Same as I-2

II-3 Convergence check: If $\sum_i (V_i^k - V_i^{limit})^2 < \varepsilon_2$, where the summation is for all PQ buses i with voltage magnitude violations, and if a gradient check as in I-3 is satisfied, the second stage converges; else, go to II-4.

II-4 Computation of $\Delta \underline{u}$: Same as I-4

II-5 Computation of stepsize limit: Find α_u as in I-5 and using the linearized relations find the limiting stepsizes α_{Qi}, α_{Qs} and α_{Vj} where the α's are as described in Section V.

II-6 Bus status switching:

(a) For every PV bus i, if $|\alpha_{Qi}\Delta Q_i| < 0.01|Q_i^{limit}|$ set $Q_i^k = Q_i^{limit}$ and change its status to PQ bus permanently.

(b) For the slack bus, if $|\alpha_{Qs}\Delta Q_s| < 0.01|Q_s^{limit}|$, set $Q_s^k = Q_s^{limit}$, change its status to PQ bus permanently, pick a new slack bus, and resolve the power flow.

(c) For every PQ bus j, if $|\alpha_{Vj}\Delta V_j| < 0.0025$, set $u_j^k = V_j^k$ and change its status to PV temporarily.

Recompute $\underline{r}$, $\Delta\underline{u}$, $\Delta\underline{x}$, α_u, α_{Qi}, α_{Qs}, α_{Vj}, restore the status of those PQ buses that are switched temporarily to PV buses back to PQ status.

II-7 Slack bus P limit: Find α_{Ps} such that $P_s^M \le P_s^k + \alpha_{Ps}\Delta P_s \le P_s^M$, If $|\alpha_{Ps}\Delta_{Ps}| < 0.05\ P_s^{limit}$, select a new slack bus, solve the power flow and go to II-2; else go to II-8.

II-8 Line search: Find $\hat{\alpha}$ that minimizes $F(x^k + \alpha\Delta x, u^k + \alpha\Delta u)$ for $0 < \alpha < \min\{\alpha_u, \alpha_{Qi}, \alpha_{Qs}, \alpha_{Vj}, \alpha_{Ps}\}$

II-9 Update: same as I-8.

FELIX F. WU received the B.S. degree from the National Taiwan University; the M.S. degree from the University of Pittsburgh, both in Electrical Engineering; and the Ph.D. degree in Electrical Engineering and Computer Sciences from the University of California at Berkeley.

From 1972 to 1974, he was an Assistant Professor with the Department of Electrical Engineering, University of Pittsburgh. Since July 1974, he has been with the Department of Electrical Engineering and Computer Sciences, University of California at Berkeley, where he is now an Associate Professor. During 1976–1977 he was on industrial leave with the Pacific Gas and Electric Company to develop methodologies for power system planning studies. He is presently a consultant to PGandE.

Dr. Wu is a member of the Computer and Analytical Methods Subcommittee and the Dynamic Performance Subcommittee of the Power System Engineering Committee, and the Power Engineering Education Committee of the IEEE Power Engineering Society. He is the chairman of the Technical Committee on Power Systems and Power Electronics, and a member of the Large-Scale Systems Committee and the Nonlinear Circuits and Systems Committee, of the IEEE Circuits and Systems Society. He is also a member of Eta Kappa Nu, Tau Beta Pi, Sigma Xi, and the American Association for the Advancement of Science.

J. F. LUINI (SM'78) received his B.S. and M.S. degrees from the University of California, Berkeley, in 1957 and 1964 respectively.

Since 1958 he has been employed by Pacific Gas and Electric Company where he has been responsible for dynamic performance computer modeling, and system analysis in the Department of Engineering Planning.

He has participated in EPRI sponsored AC/DC research, and has served on the steering committees of a number of other EPRI dynamic performance research projects.

He is presently a Senior Control System Engineer in the Dynamic Analysis Performance section.

He is a member of the IEEE Control Systems Society, and Power Engineering Society with membership on the Computer and Analytical Methods, Excitation Systems, and System Dynamic Performance Subcommittees.

He is also Chairman of the WSCC Systems Modeling Task Force.

GEORGE GROSS (M'75) was born in Cluj, Romania. He was graduated from McGill University in Montreal, Quebec with a B. Eng. (Hons) in Electrical Engineering. He continued his studies at University of California at Berkeley where he was awarded the M.S. and Ph.D. degrees in Electrical Engineering and Computer Sciences. During his graduate work at Berkeley he was a Research Assistant with the Electronics Research Laboratory, doing research in the areas of optimization, nonlinear control and power systems.

Dr. Gross joined the Engineering Computer Applications Department of Pacific Gas and Electric Company in 1974. He is in charge of directing and conducting work involving the investigation, evaluation and development for computer implementation of new mathematical techniques and analytical engineering methodology for solving problems arising in power system planning, operation and control. Dr. Gross is a Senior Computer Application Engineer with the utility.

Dr. Gross has taught graduate level courses in power systems planning and operations at the University of Santa Clara, California, the Center for Professional Advancement, New Jersey and the University Extension, University of California, Berkeley.

George Gross is a member of the Computer and Analytical Methods Subcommittee of the Power Systems Engineering Committee of the IEEE Power Engineering Society. He is a member of the 1979 PICA Technical Committee.

PUI MEE LOOK (M'75) received the B.S. and M.S. degrees in Electrical Engineering and Computer Sciences from the University of California, Berkeley, California in 1971 and 1972, respectively.

She joined the Pacific Gas and Electric Company, San Francisco, California, in 1972. She is a Computer Application Engineer in the Systems Engineering Group of the Engineering Computer Applications Department. Her work is in the areas of load flow, dynamic stability and optional load flow.